Simulation of growth of Ni-Zr interfacial amorphous regions under nonequilibrium conditions

P. Mura, P. Demontis, and G. B. Suffritti
Dipartimento di Chimica, Università di Sassari, Via Vienna 2, 07100 Sassari, Italy

V. Rosato and M. Vittori Antisari
Comitato Nazionale per la Ricerca e per lo Sviluppo dell'Energia Nucleare e delle Energie Alternative, Centro Ricerche Energetiche della Casaccia, Settore Nuovi Materiali, Casella Postale 2400, 00100 Rome, Italy

(Received 22 November 1993; revised manuscript received 25 March 1994)

We have simulated the response of an interfacial amorphous region formed between nickel and zirconium lattices upon temperature increase or the application of uniaxial load by means of molecular-dynamics simulation of a model system based on an n-body potential. The behavior of the amorphous region has been investigated as a function of the load intensity and duration. The system reacts upon uniaxial load application with the growth of the amorphous interface. This has been related to the structural change occurring in the glassy region in the form of a density variation consequent to the introduction of excess free volume. These findings are qualitatively consistent with the current hypothesis invoked to explain diffusion and growth of interfacial amorphous regions formed upon load application on bulk diffusion couples.

INTRODUCTION

The effects of nonequilibrium conditions on the formation and growth of amorphous structures have been the object of a lively debate following the widespread use of alloying techniques where solid-state amorphous reactions (SSAR) among metallic systems can occur (see Refs. 1–4).

The picture of the formation of an amorphous structure in the SSAR resulting from the unlimited grains refinement through plastic deformation (leading to scattering volume elements of subnanometers size whose diffraction contrast becomes indistinguishable from that of an amorphous structure) has been severely criticized and rejected.[5] However, whereas the atomistic mechanisms of amorphous formation through "classical" techniques, such as vapor quenching and splat cooling, are well understood, the outcomes of alloying techniques such as interdiffusion in thin films at equilibrium[6] or under nonequilibrium conditions[3,7] have addressed several questions concerning both the nucleation of the amorphous structures at the interface and the growth of those regions under the effects of temperature, applied load and/or concentration gradients. In this framework theoretical and experimental research concentrated a great deal of efforts to pursue a better understanding of the microscopic mechanisms of the amorphization process at the solid state (see Refs. 4 and 8).

Let us consider the interface between Ni and Zr single crystals. A nucleation barrier exists for the reaction of the two metals which is related to the presence of a strong strain energy associated with the exchange of a Ni atom for a Zr atom in the Zr lattice (and vice versa) and it is only partially lowered by the mixing enthalpy and the increase of configurational entropy.[9] At $T=500$ K, even taking into account the highest possible value of the mixing enthalpy between Ni and Zr, the equilibrium concentration of exchanged pairs is almost vanishing. The reaction of Ni/Zr coupled at low or intermediate temperatures can be increased providing appropriate heterogeneous nucleation sites such as grain boundaries[7] or other crystal defects. This can be achieved by several means: by reacting polycrystal and single-crystal interfaces at intermediate temperatures,[7] by irradiating the interface[10] or by means of polycrystalline interfaces submitted to severe plastic deformations at room temperature.[3] By these means, the formation of a reacted region, in most cases exhibiting an amorphous structure, can be achieved.

In this work we disregard the problem of nucleation of the amorphous phase at the interface. Following Highmore,[9] we take over the limits of the classical nucleation theory by considering the initial reaction at the Ni/Zr interface as being related to the formation of a solid solution obtained by exchanging Ni atoms for Zr atoms in the Zr lattice (and vice versa). The creation of such solid solution could ideally mimic the result of the atomic recombination subsequent, say, to interface irradiation.[10]

We would rather focus on the problem of the amorphous phase growth both in equilibrium or under the effects of applied nonequilibrium conditions (i.e., external loads). Experimental results on the growth rate of amorphous layers have shown that, in most cases, the reaction is controlled by diffusion through the already formed glass. The problem that we address in this paper is related to the effect of external perturbations on the atomic transport through the interface layer.

If we refer to the results of plastic deformations of diffusion couples,[3] experimental results showed an unusually fast growth of the amorphous interlayer; this phenomenon has been interpreted as being caused by a considerable enhancement of diffusion processes during

0163-1829/94/50(5)/2850(8)/$06.00

the deformation time, resulting from the applied strain and affected also by the strain rate. Indeed, the temperature increase necessary to explain the measured diffusion enhancement is very much larger than that effectively measured. As, in that experiment, the deformation and the growth of the amorphous region occur simultaneously, it is very difficult to test directly the connection with a modelization of the effect[11] developed in the frame of the "free volume model."[12] In any case the relative role of the increase of temperature and of density of diffusion carrying defects on the diffusivity enhancement due to plastic deformation is a subject of different interpretations.[4] In the elastic limit, the application of tensile stress on the plane parallel to the interface in a multilayered structure resulting from the growth on different substrates, leads to a lowered activation barrier for diffusion along the composition gradient.[6] The same effect should be induced by the application of compressive load perpendicular to the interface in the range of the "Bridgman regime" ($P > 10^8$ Pa).[13]

The common feature resulting from the application of the mentioned nonequilibrium conditions is to introduce into the system a certain amount of "excess free volume" (EFV hereafter) defined as an excess volume per atom with respect to that pertaining to the system under equilibrium conditions, as shown by Cahn *et al.*[14] A recent molecular-dynamics simulation[15] has evidenced the role played by EFV in enhancing diffusion processes in glasses. In that work, a given localized source of EFV was created in an amorphous system by removing one or more particles; the subsequent relaxation process was then followed on isothermal constant pressure or constant volume conditions. In both cases, two different regimes have been detected during the relaxation process: (1) a fast one, with low activation energy (~ 0.1 eV), which involves a rapid redistribution of the localized EFV to the entire system and (2) a slow one, with higher activation energy (~ 1 eV), which accounts for the search of a new equilibrium condition. The fast regime is effective at low temperatures when thermal annealing does not allow a rapid shrinkage of the EFV. However the role of this mechanisms on the value of the macroscopic effective interdiffusion coefficient, which is supposed to be connected to the concentration of EFV fluctuations large enough to support atomic jumps, has not yet completely ascertained.

In this work we have studied the effects of the applied load as we have followed the response of an amorphous interface, created between a Ni and a Zr lattices, to the application of an uniaxial, compressive load in the direction perpendicular to the interface. The purpose is to simulate an experimental setup similar to that reported in Ref. 3 and to verify the microstructural aspects of the fast amorphous phase growth induced by plastic deformations. Due to the single-crystal structure and the geometrical arrangement of the used model system (which will be described in the next section) the yield point for dislocation creation and displacement is higher than that of a polycrystalline sample. Our quantitative results must be thus considered as an upper bound relative to the corresponding experimental test.

MODEL AND COMPUTATIONS

The model used for computations consists of a Ni lattice ($N_1 = 600$ atoms arranged in the fcc structure with a stacking sequence of six [111] atomic planes along the z direction) and a Zr lattice ($N_2 = 640$ with hcp structure consisting of ten [100] layers). An interface is thus created along the z direction. The dimension of the xy section of the lattices have been chosen large enough to minimize the mismatch effects between the two surfaces. Periodic boundary conditions have been imposed along the x and y directions according to the Zr lattice dimensions. Along the z direction, periodic boundary conditions do create another interface. Only one of the resulting interfaces will be disordered and considered for computational purposes.

The misfit introduced between the Ni lattice dimensions and the periodic conditions along the x and y directions lowers the Ni density of $\sim 1.8\%$ (with respect to that of a bulk system at the same temperature). This value must be compared to density decrease at the melting point which is $\sim 10\%$. However, we have directly verified that the resulting reduced density of the Ni crystal does not introduce spurious effects on its thermodynamic behavior other than those recorded in the high-temperature range (leading to anticipated melting). We have thus confined our analysis at temperatures as low as $T \leq 0.5 T_m$ (where T_m is the melting temperature).

Atoms interact via a many-body potential derived from a second-moment approximation of a tight-binding Hamiltonian[16] extended to high-order neighbors.[17] The used potential parameters describing the Ni-Zr interactions are those originally introduced by Massobrio, Pontikis, and Martin.[18] Simulations have been carried out in the constant stress-constant temperature (Nose-Parrinello-Rahman) ensemble. A fifth-order predictor-corrector algorithm with a time step $\tau = 2 \times 10^{-15}$ s has been used to integrate the equations of motion.

The creation of the interface has been performed by approaching the two lattices at different distances (along the z direction), allowing the system to relax and then recording the enthalpy as a function of the different imposed z separation. A minimum enthalpy value has been found at a given z separation which has been thus retained to define the starting configuration. The density profile of each species along the z direction $\rho_\alpha(z)$ in the relaxed configuration of the interface at $T = 500$ K, obtained after several picoseconds of relaxation at $P_{\text{ext}} = 0$, is drawn in Fig. 1. The evaluation of $\rho_\alpha(z)$ allows, furthermore, to define the position of the single atomic layers enabling the evaluation of local (i.e., restricted to the single layer) thermodynamic and structural properties.[19]

Interfacial disorder has been created by exchanging the positions of a certain number of Ni atoms with those of an equal number of Zr atoms in one of the two interfaces created via periodic boundary conditions. Only atoms belonging to the first two layers closer to the interface of each lattice have been displaced. The amount of disorder introduced at the interface has been quantified by a density value κ defined as the ratio between the total number of exchanged atoms and the total number of atoms be-

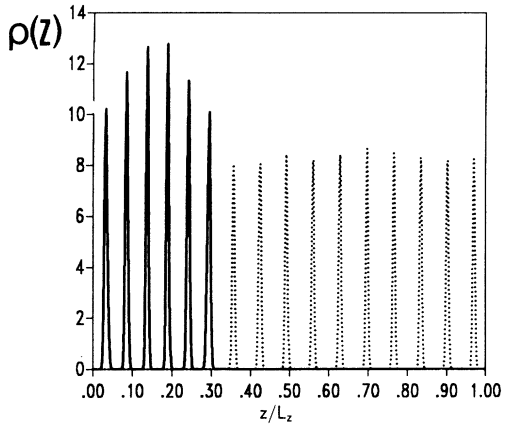

FIG. 1. Density profile $\rho_\alpha(z)$ along the z direction for the unperturbed model system at $T=500$ K (α=Ni,Zr). $\rho_{Ni}(z)$=full line; $\rho_{Zr}(z)$=dotted line. Abscissa is expressed in scaled coordinates, ordinates in arbitrary units.

longing to the first two atomic layers (200 Ni and 128 Zr).

To compare the results obtained in the interfacial region with those pertaining to an amorphous structure, we have simulated the thermodynamics properties of a "true" amorphous state obtained by quenching down to $T=500$ K a Ni-Zr system (containing an equal number of Ni and Zr atoms as the considered interfacial region) molten at $T\sim2000$ K after an homogenizing relaxation lasted several tens of picoseconds. The amorphous reference system has been simulated surrounded by usual periodic boundary conditions. The thermodynamic and structural values relative to the reference amorphous state, which will be referred to in the following, have been evaluated on this system. Fig. 2 reports the total radial distribution function of such a reference state.

The response of the interface has been evaluated at different values of κ after the relaxation run lasted several tens of picoseconds. In Figs. 3(a) and 3(b) we report the behavior of the volume V_λ and the potential energy of the interfacial region as a function of κ. The volume V_λ of the region affected by the disorder has been evaluated by multiplying the xy section of the sample (as deduced by the average values of the **h** metric tensor[20]) times the distance between the points (as those marked A and B in Fig. 4) which indicates the minima of the $\rho_\alpha(z)$ preceding the two layers of each species affected by the particles exchange. The potential energy value reported in Fig. 3(b) refers to local averages over V_λ. In Figs. 3(a) and (b), the corresponding values pertaining to the amorphous reference state have been drawn (dotted lines). Figure 5 reports an y-z projection of a snapshot of the whole sample (white particles are zirconium atoms, shaded particles are nickels) for $\kappa=0.33$ at the end of equilibration procedure. This configuration corresponds to the density distribution $\rho_\alpha(z)$ drawn in Fig. 4. Arrows, in Fig. 5, mark the extension of the amorphous region defined in Fig. 4 by points A and B.

For $\kappa>0.20$ the potential energy per atom at the interface has the same value of that pertaining to the amorphous reference state, with a $\Delta U/U\sim1.6\%$ with respect to the crystalline interface configuration [i.e., the relaxed interface before the atoms exchange, Fig. 3(a)]. The specific volume of interface particles is, in turn, always smaller than that relative to the amorphous reference state, even for $\kappa>0.20$ [Fig. 3(b)]. In order to establish the real structure of the disordered interfacial region we

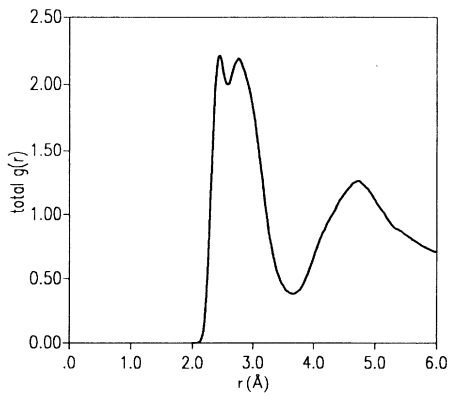

FIG. 2. Total radiation distribution function for the amorphous reference state (a-$Ni_{200}Zr_{128}$ at $T=500$ K and $P_{ext}=0$).

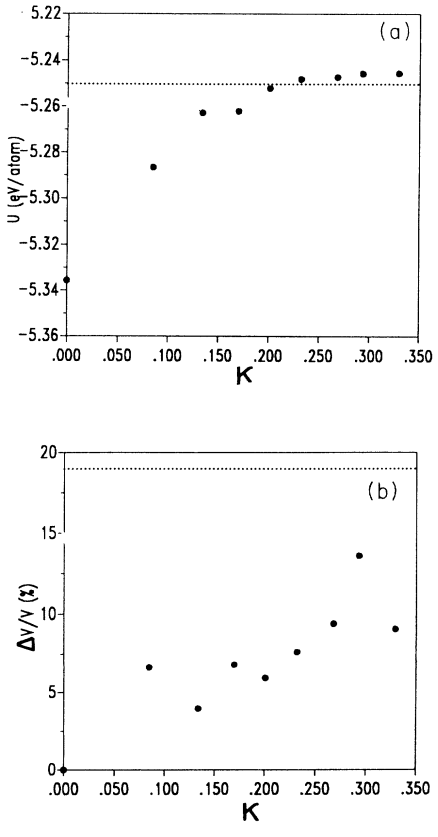

FIG. 3. (a) Internal Energy variation of the glassy layer as a function of κ (density of the exchanged atoms); (b) volume variation of the glassy layer as a function of κ. In both figures, the dotted line represents the value of the considered quantity in the reference amorphous phase (see text).

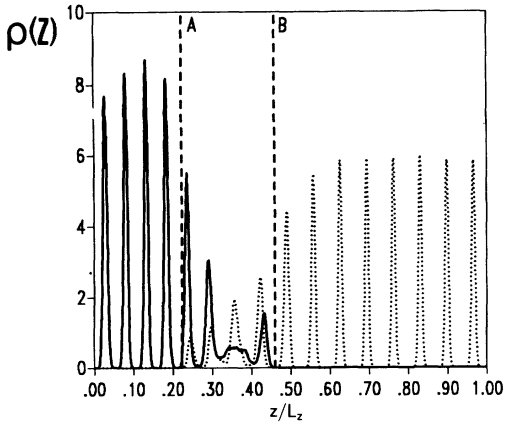

FIG. 4. Density profile $\rho_\alpha(z)$ at $T=500$ K for $\kappa=0.33$ (same conventions of Fig. 1). A and B mark the extent of the disordered region (which corresponds to the region between the arrows of Fig. 5).

have evaluated its total radial distribution function which appears (Fig. 6) very similar to that reported in Fig. 2, pertaining to the reference amorphous state. The only sensible difference between the two distributions is due to a residual short-range order surviving in the Ni-Ni distribution. This effect could be related to the presence of crystalline boundaries which bound the disordered interface region and squeeze its structure, thus inhibiting a complete relaxation of the region along the z direction (at least for times of the order of the simulation times).

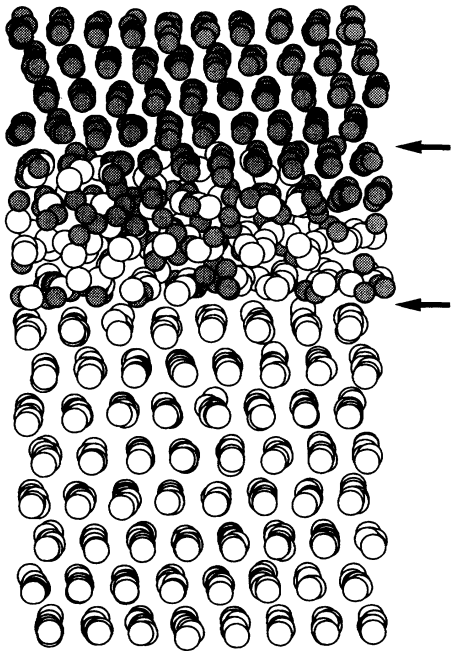

FIG. 5. Snapshot of the system configuration after the introduction of disorder ($\kappa=0.33$) and a relaxation lasting several tens of picoseconds (white atoms are zirconiums, shaded particles are nickels). Arrows indicate the extent of the disordered region.

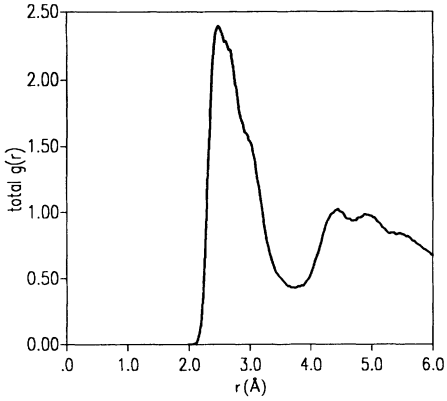

FIG. 6. Total radial distribution function for the relaxed interface with $\kappa=0.33$.

The main purpose of this work is to study the role of the EFV in onsetting efficient diffusion and growth in amorphous systems. We have considered two different methods to increase the free volume of a sample: (a) by increasing the system temperature; (b) by applying an external perturbation as, for instance, a stress field. In the following we report the results obtained upon the application of both these perturbations and we compare the relative effects induced on a given system (that with an interfacial disorder indicated by $\kappa=0.33$).

EFFECTS OF TEMPERATURE

We have warmed the system up to $T=750$ and 900 K without applying any external pressure (i.e., $P_{xx}=P_{yy}=P_{zz}=0$). At $T=750$ and 900 K we have evaluated $\lambda=8.90$ and $\lambda=9.21$ Å, respectively, (whereas $\lambda=8.68$ Å at $T=500$ K). The increase of V_λ in both cases leads to an effective expansion coefficient $\alpha'=\Delta V_\lambda/V_\lambda/\Delta T\sim 1.5\times 10^{-4}\ \mathrm{K}^{-1}$ (whereas the thermal expansion of a "true" amorphous system of the same composition should have been of the order $\alpha\sim 10^{-5}$ K^{-1}).

Starting from the $T=900$ K final configuration we have quenched the system down to $T=500$ K in order to establish if we are in presence of a growth of glassy phase or of an anomalous thermal effect. The structure and the thermodynamic properties relative to the configuration at $T=500$ K, obtained after 20 ps of relaxation, are very similar to those pertaining to the starting $T=500$ K region. The short-time-scale reversibility of the observed process, therefore, does not allow its description in terms of a true growth process. The observed thermal expansion should be, in this case, related to some proximity effect due to the presence of the bounding crystalline phases. However, owing to our method of measuring λ, we cannot exclude that the observed expansion could be related to some anomalous atomic oscillation at the interface. It has to be noticed that the diffusion coefficient of amorphous NiZr at 900 K extrapolated from experimental data is around 4×10^{-11} cm^2/s.[21] corresponding to the jump of some atoms over 10^3 in the explored time interval. In conclusions, our results are coherent with the

experiments showing that growth process of the amorphous interface upon temperature increase is determined by the mechanisms of diffusion in the amorphous phase, characterized by diffusion coefficients which are not measurable in the time scale of a computer simulation and activation energies as high as some eV. Raising the temperature induces only a moderate, delocalized increase of the free volume available for diffusion as vacancy-formation energy still persists on values of some eV.

EFFECTS OF THE UNIAXIAL LOAD

The efficiency of mechanical deformation in determining the increase of free volume via an ease of vacancy formation has been discussed in the case of crystalline Ni_3Al (in its $L1_2$ and $A1$ phases).[22] In that case, a considerable decrease of vacancy-formation energy has been detected in a system where hydrostatic compression was applied. We can thus expect a similar behavior for the disordered structure with a lowering of the formation energy of vacancylike defects with a consequent increase of their concentration. This fact should have two consequences: first, the enhancement of the effective diffusivity and second, the increase of the average EFV. On the other hand, this increase can give rise to a larger vacancy concentration in metastable equilibrium.[13,24]

The response of the system under the action of a compressive load has been simulated by applying to the model and external stress along the z direction perpendicular to the interface, using a step-wise function characterized by an intensity L and a duration Γ. Load strength and duration seem to be more effective in determining the response of the system with respect to, for instance, the shape of the applied perturbation. We have thus adopted a simple perturbation function (a step function) of two different durations: the first, $\Gamma_1=2$ ps, supposed to be of the same order of magnitude of relaxation processes, the second, $\Gamma_2=20$ ps, ten times longer, which allows the system to pursue its relaxation under the persistent effect of the load.

After the load removal, the system has been further left free to relax for several tens of picoseconds. Its behavior has been recorded during both the loading and the relaxation periods. For each duration, we have performed several simulations with loads ranging up to a critical value L_c related to the yield strength of the system. The critical value was detectable as related to a severe, irreversible compression of the whole system along the load direction, resulting in the complete distruction of the residual order even in the crystalline regions of the system.

In the case of the unperturbed disordered interface, the local analysis has been performed by averaging the relevant quantities over the set of particles belonging to each atomic layer defined on the basis of $\rho_\alpha(z)$, as previously stated. After load application, however, a straightforward recognition of atomic layers on the basis of $\rho_\alpha(z)$ was not always possible. In such cases, the extension λ of the perturbed interface region along the z direction has been defined as the difference between the z position of the first Zr atom (i.e., the one with the lowest z coordinate) and that of the last Ni atom (i.e., that with the highest z coordinate) detected during the entire simulation run. Accordingly, the amorphous region volume V_λ has been evaluated by multiplying λ times the interfacial area.

In our simulations we have found that the critical load L_c decreases with increasing the load duration Γ_c. We have found $L_c=160$ kbar for $\Gamma_1=2$ ps and $L_c=110$ kbar for $\Gamma_2=20$ ps. This phenomenon (stress-induced melting) has been recently described in paper by Blumberg *et al.*[23] In that work, stress-induced failure of perfect solids has been simulated as a function of strain rate and temperature. The authors have shown that, under slow strain rates and low temperatures, system failure can be, sometimes, preceded by a solid-solid phase transformation. In the high-temperature range, in turn, any solid rearrangement seems to be inhibited and direct failure is observed via a stress-induced melting.

In our work we have, instead, imposed a sudden compressive load up to the critical value ($P_{xx}=P_{yy}=0$, while $P_{zz}=L$ with L in the range 10–200 Kbars) removed after an application period Γ. We have studied the cases $\Gamma_1=2$ ps for $L=150$ kbar and $\Gamma_2=20$ ps for $L=100$ kbar. In all cases the temperature of the system has been kept constant at $T=500$ K. Using this procedure the applied strain rate results to be much larger (of several orders of magnitude) than that applied in Ref. 23. However, although imposing a stress rather than a strain (as done in Ref. 23), we have verified that our system is able to respond elastically to the applied stress. We have, in fact, evaluated the externally applied force, defined as $F_{\text{ext}}(t)=P_{zz}\cdot S(t)$ [where $S(t)$ is the instantaneous values of the interfacial area] and the internal force, defined as $F_{\text{int}}(t)=\sigma_{zz}(t)\cdot S(t)$ [where $\sigma_{zz}(t)$ is the instantaneous value of the stress tensor in the direction perpendicular to the interface]. Figures 7(a) and 7(b) report the time behavior of $F_{\text{ext}}(t)$ and $F_{\text{int}}(t)$ as a function of time during the load application (a) $L=150$ kbar and $\Gamma=\Gamma_1$, (b) $L=100$ kbar and $\Gamma=\Gamma_2$. Despite an initial strong deviation from linearity, at longer times (of the order of less than 20% of the load duration) the system reaches an elastic response regime [which is even more clearly shown in Fig. 7(b)].

Figures 8(a) and 8(b) show the volume of the disordered region λ, its number density and the total length of the system as a function of the time elapsed from the application of an external stress up to a complete relaxation for the Γ_1 and Γ_2 time durations (with the respective loads $L=150$ kbar and $L=100$ kbar), respectively. It is possible to observe that the total volume of the sample exhibits, in both cases, a monotonic shrinkage during the load application. The original volume is, however, fully recovered upon the removal of the external pressure as in a typical elastic transient without a permanent shear of the structure.

A completely different behavior is shown by the disordered region. After a short elastic transient clearly evidenced in the Γ_1 case, one can observe a permanent growth of the disordered layer which is more evident in

the Γ_1 case despite the shorter duration of the deformation event, thus pointing out the dominant role of the deformation parameters on the growth of the disordered region. This effect, which underlines the activated nature of the growth mechanism, is consistent with the picture that growth depends on the availability of EFV. It is the deformation strength, rather than its duration, which can provide to the system the energy required for reducing the vacancies formation energy thus increasing their concentration. Duration could be uneffective if some threshold energy, necessary to significantly reduce the energy for vacancies formation, is not provided to the system. Figure 9 shows the density profile along the z direction of the system at equilibrium after the compression and the subsequent relaxation in the case $\Gamma_1=2$ psec, $L=150$ kbar. Figure 10 shows a snapshot of the resulting structure.

The density reduction of the amorphous region upon mechanical deformation is not surprising. Recently Cahn *et al.*[14] reported density measurements of metallic glasses under the effect of thermal annealing or plastic deformations. They found in $Pd_{77.5}Cu_6Si_{16}$ a density decrease $\Delta\rho/\rho=-0.14\%$ upon rolling reduction of 30–40 %. Although it has been argued that plastic deformation increases the homogeneity of the glass via, for instance, the removal of microporosity, it is conceivable that the free volume disappearance is related to some defects produc-

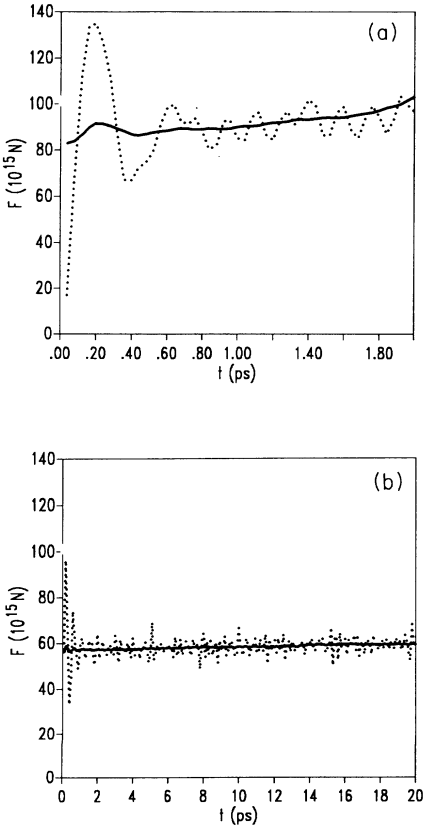

FIG. 7. Time behavior of external and internal forces which develop in the model system during the load application. Full line=internal force, dotted line=external force (a) $L=150$ kbar, $\Gamma=2$ ps; (b) $L=100$ kbar, $\Gamma=20$ ps, ($T=500$ K).

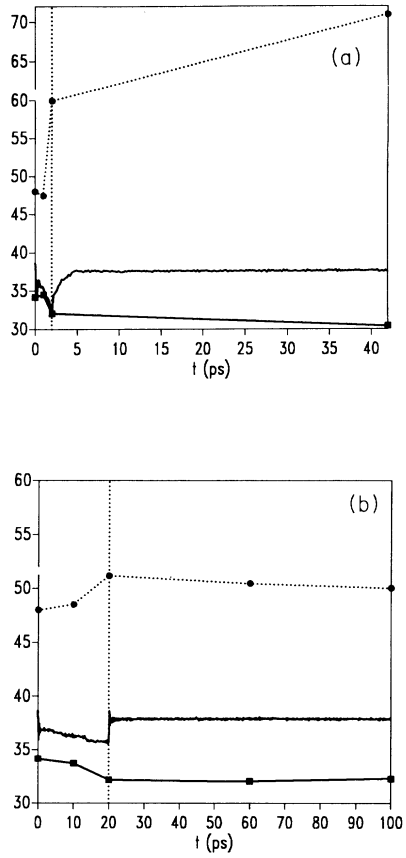

FIG. 8. Time variation, at $T=500$ K, of the overall z length of the model, in Å (continuous line); volume of the amorphous region expressed in $Å^3/100$ (full circles) and density of the amorphous region expressed in $500/Å^3$ (full squares) (a) $L=150$ kbar, $\Gamma=2$ ps; (b) $L=100$ kbar, $\Gamma=20$ ps (the choice of the units in these figures has been driven by the requirement to fit the three curves in the same plot).

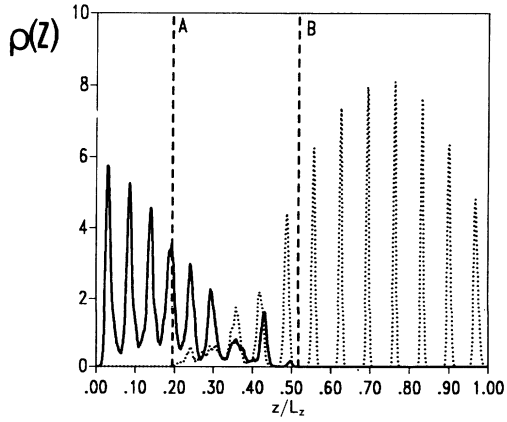

FIG. 9. Density profile $\rho_\alpha(z)$ at $T=500$ K for $\kappa=0.33$ for the system after the application of the load $\Gamma=\Gamma_1$ and $L=150$ kbar and a relaxation lasting 80 ps (same conventions of Fig. 1).

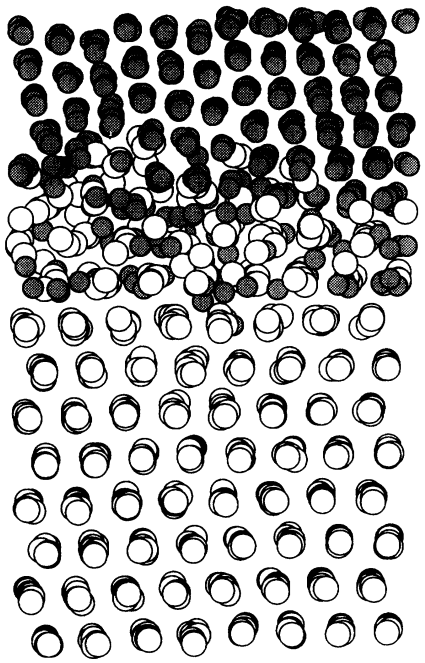

FIG. 10. Snapshot of the system configuration ($\kappa=0.33$) after 80 ps of relaxation subsequent to the application of the perturbation with $L=150$ kbar, $\Gamma=2$ ps. White atoms are zirconiums, shaded particles are nickels.

tion at the crystal-glass interface. Moreover, experimental evidences[14] have indicated that free volume created by deformation diffuses progressively away from the shear bands (which, in our model system, could be assimilated to the regions where stress intensification occurs) aided by the diffusivity increase, up to assuming a final distribution which is intermediate between complete uniformity and total localization.

A comparison with the experimental situation is not straightforward owing to the different ranges of stress and duration time explorable with the two methods. Moreover the experiments have been carried out in the plastic regime with a noticeable permanent strain of the whole sample. However, we can notice that the experimental results have shown a well-defined exponential relationship between the thickness of the amorphous layer after deformation and the strain resulting from the plastic deformation itself with a minor role played by the duration of the deformation experiment,[11] in agreement with our arguments.

It is interesting to notice that the growth process appears to continue even after the removal of the external stress. Thus it is shown that the enhanced transport properties of the glassy layer seem to be more related to some structural change of this phase induced by the deformation (which appears to recover when the structure is left free to relax with characteristic times larger than the deformation ones we have explored) than to some effect directly related to the application of the external pressure.

In order to ascertain possible correlations between atomic transport mechanisms and structural changes, we have reported the behavior of the amorphous layer number density δ defined as the ratio between the particles contained in the amorphous layer (as deduced by the $\rho_{Ni}(z)$ and $\rho_{Zr}(z)$ integration between the limiting edges of the amorphous zone) and its volume. A density variation of the disordered phase is indeed observed during the simulated experiment [as reported in Figs. 8(a) and 8(b)], whose behavior appears to be correlated with the growth process. In fact, the fast amorphous phase growth appears to occur simultaneously with the onset of a density reduction, while detectable atomic transport seems to occur after the loading period until δ keeps anomalously low values.

This can support, even if in a qualitatively way, the phenomenological picture that high mobility is related to the presence of EFV in the amorphous structure[11] and that the EFV can be introduced by plastic deformations.[23] We have estimated the diffusion coefficients via the evaluation of the average mean-square displacement $\langle r^2(t)\rangle$ during the load application. The diffusivities measured during the application of the load are of the order of 10^{-4} cm^2/s for the Γ_1 case and 10^{-5} cm^2/s for the Γ_2 one, while they reduce, in both cases, to values lower than 10^{-8} cm^2/s after the load removal. The diffusivity values under compression are higher by several orders of magnitude than those which can be obtained experimentally by deforming bulk diffusion couples, pointing out again that a quantitative comparison between simulations and experiments in this field is far beyond the capabilities of the present computing machines. However our work has been able to show that the main assumptions at the basis of the phenomenological models able to describe this kind of effect are indeed recovered in an atomistic simulation. In fact, the original hypothesis that diffusivity in amorphous alloys is depending on the amount of EFV in the structure seems to be quite coherent with the results of our simulation. Moreover, the increase of both the EFV and the diffusivity appears to onset at the same time after the application of the external load. We can suppose, in agreement with the original hypothesis of Spaepen[24] that this can be correlated with some atomic jumps induced by the external load.

CONCLUSIONS

The main findings of the simulations can be summarized as follows. After some time from the application of the load both the EFV and atomic mobility in the amorphous interlayer begin to increase. We observe a permanent growth of the amorphous interlayer which is strictly related to the density reduction in the structure and keeps going until a complete recovery of the original density of the glassy phase.

The basic assumption of macroscopic models developed to describe the fast growth of the amorphous interlayer[3,11,24] are completely coherent, even if in a qualitative way, with the results of a simulation carried out starting from the interaction potentials.

ACKNOWLEDGMENTS

The authors kindly acknowledge Dr. Carlo Massobrio for useful comments and suggestions.

[1]M. L. Trudeau, R. Schultz, D. Dassault, and A. VanNeste, Phys. Rev. Lett. **64**, 99 (1990).
[2]L. Schultz, J. Less Common Met. **145**, 233 (1988).
[3]G. Mazzone, A. Montone, and M. Vittori Antisari, Phys. Rev. Lett. **65**, 2019 (1990).
[4]W. L. Johnson, in *Materials Interfaces,* edited by D. Wolf and S. Yip (Chapman & Hall, London, 1992), p. 516.
[5]D. Kulhmann-Wilsdorf and M. S. Bednar, Scr. Met. Mater. **28**, 371 (1993).
[6]N. Karpe, K. Kyllesbech, and J. Bottiger, Philos. Mag. B **66**, 507 (1992).
[7]A. M. Vrendenberg, J. F. M. Westendorp, F. W. Saris, N. M. van der Pers, and Th. H. de Keijser, J. Mater. Res. **1**, 774 (1986).
[8]D. Wolf, P. R. Okamoto, S. Yip, J. F. Lutsko, and M. Kluge, J. Mater. Res. **5**, 286 (1990).
[9]R. J. Highmore, Philos. Mag. B **62**, 455 (1990).
[10]L. Thomé, T. Benkaulal, J. Jagielski, and B. Vassent, Europhys. Lett. **20**, 413 (1992).
[11]G. Mazzone, A. Montone, and M. Vittori Antisari, Scr. Met. Mater. **28**, 821 (1993).
[12]D. Turnbull and M. H. Cohen, J. Chem. Phys. **52**, 3038 (1970).
[13]V. V. Bogdanov, V. I. Kibets, L. N. Parystkaya, A. A. Puzanova, E. P. Sorokina, and M. I. Cherakov, Phys. Status Solidi A **136**, 81 (1993).
[14]R. W. Cahn, N. A. Pratten, M. G. Scott, H. R. Sinning, and L. Leonardsson, in *Rapidly Solidified Metastable Materials,* edited by B. H. Kear and B. C. Giessen, MRS Symposia Proceedings No. 28 (Materials Research Society, Pittsburgh, 1984), p. 241.
[15]V. Rosato and F. Cleri, J. Non Cryst. Solids **144**, 187 (1992).
[16]V. Rosato, M. Guillopé, and B. Legrand, Philos. Mag. A **59**, 251 (1989).
[17]F. Cleri and V. Rosato, Phys. Rev. B **48**, 22 (1993).
[18]C. Massobrio, V. Pontikis, and G. Martin, Phys. Rev. Lett. **62**, 1142 (1989).
[19]V. Rosato, G. Ciccotti, and V. Pontikis, Phys. Rev. B **33**, 1860 (1986).
[20]M. Parrinello and A. Rahman, J. Appl. Phys. **52**, 7182 (1981).
[21]G. Mazzone, A. Montone, and M. Vittori Antisari, in *Phase Transformation and Kinetics in Thin Films,* edited by M. Chen, M. O. Thompson, R. Schwartz, and M. Libera, MRS Symposia Proceedings No. 230 (Materials Research Society, Pittsburgh, 1992), p. 27.
[22]F. Cardellini, F. Cleri, G. Mazzone, A. Montone, and V. Rosato, J. Mater. Res. **8**, 2504 (1993).
[23]R. L. Blumberg Selinger, R. M. Lynden-Bell, and W. M. Gelbart, J. Chem. Phys. **98**, 808 (1993).
[24]F. Spaepen, Acta Metall. **25**, 407 (1977).

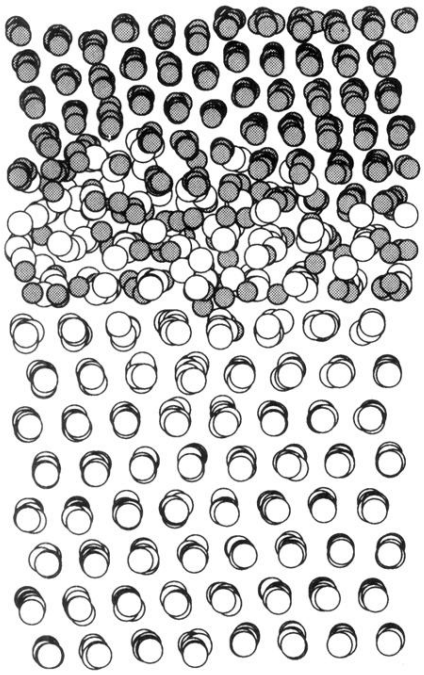

FIG. 10. Snapshot of the system configuration ($\kappa = 0.33$) after 80 ps of relaxation subsequent to the application of the perturbation with $L = 150$ kbar, $\Gamma = 2$ ps. White atoms are zirconiums, shaded particles are nickels.

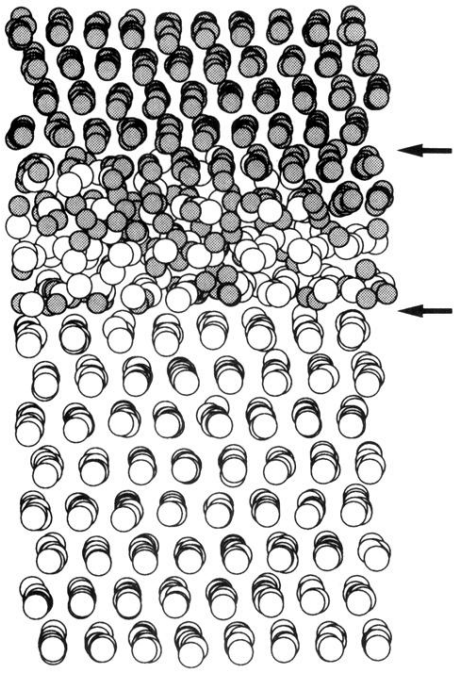

FIG. 5. Snapshot of the system configuration after the introduction of disorder ($\kappa=0.33$) and a relaxation lasting several tens of picoseconds (white atoms are zirconiums, shaded particles are nickels). Arrows indicate the extent of the disordered region.